Molecular Modeling of Bulk Impurity Segregation and Impurity-Mediated Crystal Habit Modification of Naphthalene and Phenanthrene in the Presence of Heteroimpurity Species

Graham Clydesdale, Robert B. Hammond, and Kevin J. Roberts*

Institute of Particle Science and Engineering, Department of Chemical Engineering, University of Leeds, Leeds LS2 9JT, U.K.

Received: November 13, 2002; In Final Form: January 30, 2003

The ability to predict particle morphology (shape) in the presence of habit-modifying impurities is of great use in allowing the optimization of growth conditions to produce a required crystal habit. Previous morphological modeling techniques developed by the authors[1,2] utilized the attachment energy method, which assumes knowledge of the solid-state structure, to simulate the shape of organic particulate solids while keeping the position of the impurity in the lattice fixed. These techniques are improved upon here by allowing the orientation of the adsorbing impurity molecule to be relaxed with respect to the intermolecular forces of the crystal bulk using a restricted molecular mechanics approach. This results in far more accurate attachment energies—and hence morphological simulations—than could be achieved before. The calculations also allow improved binding energies for additives in different crystal faces to be ascertained; these can be used as a measure of the equilibrium impurity segregation coefficient for liquid/solid solidification. The method is illustrated by considering the morphological impact of a variety of host/additive systems, including naphthalene doped by biphenyl and phenanthrene crystallizing in the presence of biphenyl or anthracene. A forward look to the development of this approach for more complex systems is also provided.

1. Introduction

Ever-tightening quality specification has led to an increased importance being attached to controlling and minimizing impurity content in modern chemical products. Such a scenario is prevalent in the speciality chemical product areas, particularly those related to pharmaceuticals, food, and electronic materials, for which regulative bodies such as the U.S. Food and Drug Administration are demanding increasingly lower levels of heteromolecular species, such as solvent and reaction side-products, in marketed products. The speciality chemicals businesses are often dominated by manufacturing processes involving complex chemical or biochemical synthetic manufacturing routes in which a wide range of intermediate and side-reaction products coexist within the process reactor with the target material. Separation and purification of the desired material is usually accomplished via a crystallization step in which molecular recognition processes at the interface between the particle surface and mother liquor act in such a way as to select the host molecular species and reject any impurity heterospecies. Thus, after crystallization, the desired product material can be recovered from the resultant particle/solution slurry via filtration, washing, and drying.

However, the intrinsic 2D nature of the crystal growth interface sometimes renders it incapable for certain crystal surfaces (*hkl*) of discriminating between the host and an impurity species. This is particularly true in cases in which the molecular functionality of an impurity matches, to a degree, that of the host. It is this simple principle that forms the basis of the mode of action of crystal habit-modifying tailor-made additives developed via the seminal work of Meir Lahav and Leslie Leiserowitz at the Weizmann Institute in Israel.[3,4]

Through the use of molecular modeling procedures, it is possible to identify the (*hkl*) faces on which impurities will adsorb, as well as to predict the habit-modified crystal morphology (shape) (see, for example, refs 1 and 2). However, the effectiveness of existing methodologies can be limited in cases in which the molecular dimensions of the additive exceed those of the host molecular species. This backdrop sets the perspective for this paper in which molecular minimization techniques are applied to ascertain the impurity's optimal binding site within the crystal lattice.

2. Computational Methodology

2.1. Molecular Modeling of Impurity-Mediated Crystal Habit Modification. In the HABIT program,[1,2] surface attachment energies (E_{att}) for a new layer (*hkl*) adsorbing onto the crystal surface can be calculated, for both pure and impurity-modified particle surfaces, by summing the nonbonded atom−atom energies (i.e., van der Waals and electrostatic forces) between the adsorbing molecules and the crystal bulk. This allows the prediction of an impurity-modified crystal morphology,[5] using the attachment energy as a measure of the relative growth rates of the crystal surfaces.[6] The slowest growing faces (those with the lowest E_{att} values) are not faceted out (see Figure 1) and therefore dominate the final crystal morphology at the expense of the smaller, fast-growing faces (high E_{att}). Simulated crystal morphologies are obtained using a classical Gibbs−Wulff polar plot[7,8] with the aid of the gnomonic projection by assuming that E_{att} is directly proportional to the center-to-face distance. For the work presented here, the "morphology card" within the molecular modeling package CERIUS[9] was used to produce images of the modeled morphologies.

As part of such a morphological modeling procedure, the compatibility of impurity species with the host crystal lattice is

* To whom correspondence should be addressed. E-mail: k.j.roberts@leeds.ac.uk. Phone: +44 (0)113 343 2400. Fax: +44 (0)113 343 2405.

10.1021/jp022423o CCC: $25.00
Published on Web 04/26/2003

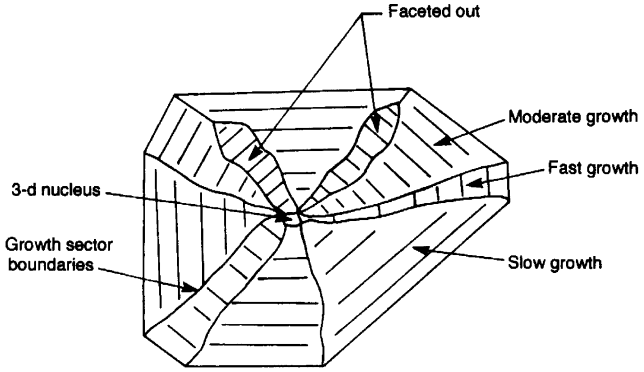

Figure 1. Schematic showing a cut made through a 3D crystal revealing its sectorial nature with crystal growth proceeding simultaneously at a number of growth interfaces.

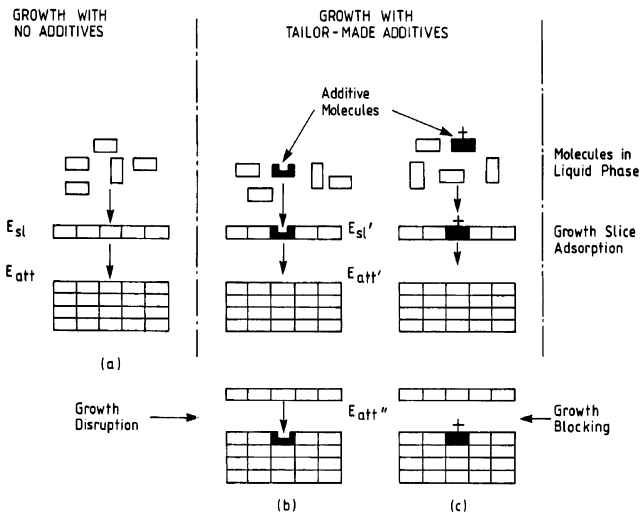

Figure 2. Schematic showing the definition of the energy terms used in morphological modeling for (a) pure systems and systems having (b) smaller than host disruptor-type additives and (c) larger than host blocker-type additives.

assessed via a calculation of the impurity's binding energy (Δb), given by

$$\Delta b = E_{\text{slice}}' + E_{\text{att}}' - E_{\text{cr}} \quad (1)$$

where

$$E_{\text{cr}} = E_{\text{slice}} + E_{\text{att}} \quad (2)$$

and the suffixes att, slice, and cr refer to the attachment, slice, and crystal lattice energies, respectively, the primed values referring to the calculation with the impurity molecule present (see Figure 2 for a visual representation of these terms).[4] A quantitative examination of the magnitude of Δb provides indicative evidence as to whether an additive may or may not absorb on a given crystal face (*hkl*)[5] (see further, section 2.2.).

However, a weakness of the binding energy criteria, as previously implemented in the HABIT program,[10−14] lies in the fact that, for a given crystal surface, Δb was calculated for an unrelaxed configuration of the impurity molecule in the host lattice. The particular configuration was derived by bringing the atoms of a submolecular moiety, present in both the host and impurity molecules, into coincidence to determine the overall position of the impurity molecule within the host lattice. This procedure was performed using conventional molecular modeling software. Hence, no allowance was made for the molecular relaxation of an impurity molecule, which may have a different size, shape, and bonding motif in comparison to a host molecule of the crystal lattice, although to some extent this was taken into account via the structured creation of molecular site vacancies as part of the impurity/host binding energy calculation. In this procedure, a vacancy (i.e., the omission of a host molecule from its lattice site) was generated where the intermolecular force calculation detected a physically unrealistic atom−atom nonbonded interaction. Without this, values for the impurity-affected attachment energies, E_{att}'' (defined in Figure 2), were large and positive and thus could not be used to produce a Gibbs−Wulff plot of the habit-modified morphology.[10] However, although the vacancy approach proved successful for simple van der Waals bonded systems[4] and allowed, for the first time, morphological simulations to be obtained directly from E_{att}'' values, experience gained during the development of HABIT95 showed in many cases that such a procedure was limited and could in some cases be quite problematic. (Note that the impurity-modified morphological simulation for naphthalene/biphenyl given in ref 1 is in error. This inadvertently repeats old data from 1994[11] in which the creation of vacancies within the crystal lattice was permitted either inside or outside the growth slice, that is, for intermolecular interactions, which contributed to either E_{sl} or E_{att}''. This oversight was corrected in the work presented in ref 12 where, as a result of a refinement of the modeling procedure, vacancies were created only outside the slice and the correct crystal simulation is given. See further, section 3.1.)

An example of this difficulty can be illustrated by a calculation of the binding energetics of doped α-amino acid systems, such as the incorporation of a larger L-alanine impurity into the smaller α-glycine host system. The vacancy generation required to fit the larger species into the host lattice removes one of the host lattice hydrogen bonds, thus significantly reducing the host/additive binding energy and producing physically unrealistic values[13] and hence simulations.

2.2. Allowing for Molecular Optimization of the Impurity Orientation within the Host Crystal Lattice. In this paper, the modeling process is further improved upon by the implementation of a more rigorous calculation methodology involving molecular relaxation of the impurity species within the host crystal lattice. For this, the existing HABIT95 code (see refs 1c and 1d) was modified via the addition of additive minimization routines allowing molecular rotations and translations, as well as intramolecular optimization using a restricted molecular mechanics approach. The details of the process employed are described below.

Initially, a single molecule of the additive material is located within a central unit cell of the crystal lattice of the host material. In the examples described in the current work, the structural similarity of the host and additive molecules enables a relatively straightforward fitting procedure to locate the starting position and orientation of the additive molecule. Through the use of the molecular modeling package INTERCHEM,[15] the common moieties of the host and additive molecule are superimposed in a procedure that minimizes the rms difference of the Cartesian coordinates of the corresponding atoms and converts the additive atom positions to fractional coordinates in terms of the host lattice. The host molecule, which is used to locate the additive, is then substituted by the additive molecule for the purposes of the optimization procedure. All of the asymmetric units of the host system within a complete unit cell are considered in turn in this procedure.

The objective function employed during optimization is the lattice energy, calculated using a nonbonded atom−atom

summation[16,17] for the additive molecule, with respect to sufficient of the surrounding host molecules (defined in terms of a radial cutoff distance) to give convergence of the lattice sum. In the work presented here, a Buckingham potential[18] with parameters from Williams[16] was used to calculate the nonbonded interactions with a simple Coulombic potential employed for electrostatic forces, fractional charges for which were calculated using the semiempirical quantum chemistry program MOPAC.[19] The minimum value of this lattice energy is sought by variation of six parameters: the rigid-body translations and rotations of the additive molecule along and about the three Cartesian axes, taking the center of coordinates of the additive molecule as the center of rotation. The first derivatives of the lattice energy with respect to the positional parameters are calculated analytically. Because the atom−atom energies are calculated in terms of the magnitude of the difference in position vector of each pair of atoms, the chain rule is employed to express the derivatives as summations in terms of the Cartesian directions. Here, the methodology follows that previously outlined by Williams.[20] The calculation of the first derivatives of the lattice energy with respect to rigid-body rotations also follows the procedure outlined in that paper. The calculation of the total differential of the lattice energy, E_{total}, is summarized in eq 3. The summation is over all pairs of atoms ij separated by a distance r_{ij}, with atom i to the limit i_{max} being in the additive molecule and atom j to the limit j_{max} being in the surrounding host molecules and where x, y, and z are displacements along the Cartesian directions, and θ_x, θ_y, and θ_z are rotations about the x, y, and z Cartesian directions, respectively. The energy

$$dE_{total} = \sum_{j=1}^{j_{max}} \sum_{i=1}^{i_{max}} \frac{dE_{ij}}{dr_{ij}} \left(\frac{\partial r_{ij}}{\partial x} dx + \frac{\partial r_{ij}}{\partial y} dy + \frac{\partial r_{ij}}{\partial z} dz + \frac{\partial r_{ij}}{\partial \theta_x} d\theta_x + \frac{\partial r_{ij}}{\partial \theta_y} d\theta_y + \frac{\partial r_{ij}}{\partial \theta_z} d\theta_z \right) \quad (3)$$

minimization is performed using a variable metric method; hence, analytical second derivatives are not calculated. The program employs the Broyden−Fletcher−Goldfarb−Shanno (BFGS) algorithm; the implementation used has been given elsewhere.[21]

In this first stage of development of the method, the positions of the host molecules surrounding the additive molecule are not allowed to relax. (The unit cell parameters are also not relaxed.) Given this restriction, the requirement for vacancies, that is, the absence of a host molecule neighboring the additive molecule, is not totally removed. Those surrounding host molecules with which bad contacts cannot be eliminated in the restricted relaxation procedure are ignored in the calculation of the lattice sum during optimization.

Optimizing the impurity orientation allows improved binding energies (Δb) to be ascertained for additives adsorbing on different crystal faces. This parameter is essentially the difference in energy between an additive molecule binding onto the growing crystal and a host molecule in the corresponding position. For a given additive molecule, Δb values of less than 10 kcal mol^{-1} were considered sufficiently low to allow impurity incorporation on these faces; here, E_{att}'' values were employed to define growth rates. For faces where Δb was considered to be too large, additives cannot bind here and host E_{att} values were used to define growth rates. Applying this procedure allows predictive calculation of the impurity-modified crystal morphology.

TABLE 1: Measured Segregation Coefficients, *K*, for a Range of Impurity Species in Phenanthrene, Together with Their Crystallographic Data[a]

material	formula	*K*	crystal system	molecular volume
phenanthrene	$C_{14}H_{10}$	host	monoclinic	244.5
fluorene	$C_{13}H_{10}$	0.95	orthorhombic	230.4
dihydrophenanthrene	$C_{14}H_{12}$	0.8	orthorhombic	250.7
dihydrothiophene	$C_{12}H_8S$	0.8	monoclinic	225.4
biphenyl	$C_{12}H_{10}$	0.5	monoclinic	215.7
anthracene	$C_{14}H_{10}$	1.6	monoclinic	237.7

[a] Taken from McArdle and Sherwood, 1985.[22a]

TABLE 2: Lattice Energy (E_{cr}) Results (kcal mol^{-1}) for Various Aromatic Hydrocarbons, Showing the Energetic Effect of the Additive Relaxation Process

material	E_{cr}
naphthalene	−19.41
naphthalene + biphenyl unrelaxed	−14.58
naphthalene + biphenyl relaxed	−15.58
phenanthrene	−24.60
phenanthrene + biphenyl unrelaxed	−20.98
phenanthrene + biphenyl relaxed	−21.03
phenanthrene + anthracene unrelaxed	−18.49
phenanthrene + anthracene relaxed	−22.29

TABLE 3: Changes in Binding Energy (Δb) and Attachment Energies (E_{att} for host, E_{att}'' for host + additive, kcal mol^{-1}) for Biphenyl Additive in a Naphthalene Crystal before and after Relaxation[a]

	+ biphenyl (unrelaxed)			+ biphenyl (relaxed)			pure host
(*hkl*)	Δb	N_V[b]	E_{att}''	Δb	N_V[b]	E_{att}''	E_{att}
$00\bar{1}$	311.91	2	−5.27	433.98	0	−6.18	−5.97
$11\bar{1}$	0.86	4	−8.01	1.06	2	−9.20	−12.24
$11\bar{0}$	1.43	3	−7.86	0.67	2	−8.30	−11.77
$20\bar{1}$	6.34	3	−10.43	12.58	1	−10.97	−13.08

[a] Results are given only for observed faces and for the asymmetric unit associated with the lowest Δb value. [b] N_V indicates the number of molecules replaced by vacancies.

Impurity/host binding energies, as calculated via this approach, can be expected to predict a more realistic estimate of impurity compatibility with both the host crystal lattice and individual crystal surface lattice planes. Such a development confers, in principle, significant benefits to the existing computational modeling methodology, in particular, increasing the accuracy of E_{att}'' and hence opening the way to more physical realism in the resultant simulations.

2.3. Modeling Bulk Impurity Segregation. A more quantitative calculation of Δb using the above technique enables, in principle, its use as a measure of the equilibrium impurity segregation coefficient, *K*, which for liquid/solid solidification is given by

$$K = C_{solid}/C_{liquid} \quad (4)$$

where C_{solid} and C_{liquid} represent, respectively, the impurity concentration in the recrystallized solid and mother liquor, respectively.[22] Thus material with $K > 1$ would be expected to have low Δb values, that is, favorable additive incorporation, and vice versa.

A useful test of this approach is that related to the purification of the aromatic hydrocarbon phenanthrene (Table 1), which clearly shows that modeling approaches based only on a correlation of host/impurity molecular volume ratio do not provide an effective measure of the segregation coefficient. A more quantitative approach, involving the calculation of host/

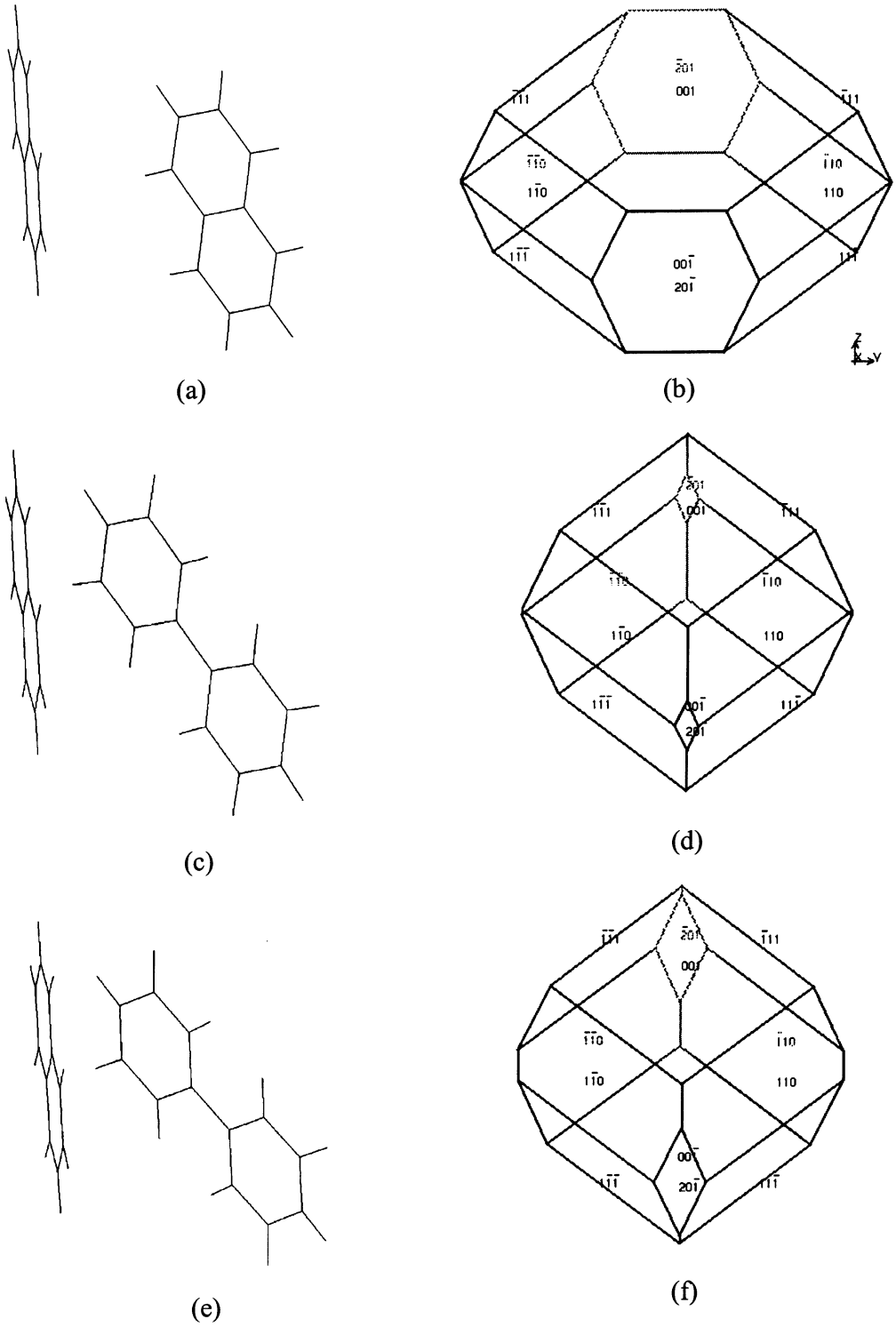

Figure 3. The effects of biphenyl on naphthalene: (a) pure naphthalene unit cell ($Z = 2$); (b) morphology of pure naphthalene; (c) unrelaxed biphenyl additive in host unit cell; (d) morphology associated with components in panel c; (e) relaxed biphenyl additive in host unit cell; (f) morphology associated with components in panel e.

impurity interaction energies following minimization, should offer a more rigorous and effective modeling methodology.

This model is tested here by considering the morphological impact and segregation coefficients of several benchmark aromatic host/additive systems, all of which crystallize in monoclinic space groups: naphthalene doped by biphenyl; phenanthrene crystallizing in the presence of either biphenyl or anthracene. Table 2 summarizes the impact on the calculated lattice energies of optimizing the position and orientation of the impurity molecule for these host/additive systems. Note that in the case of the host/additive systems the lattice energy calculation employs an additive molecule as the central reference molecule in the atom−atom summation.

3. Calculation Results and Discussion

3.1. The Effect of Biphenyl Impurity on the Naphthalene Crystal Morphology. The observed morphological impact of biphenyl (taking crystal data from ref 23) on naphthalene crystals (crystal data from ref 24) is to increase the importance of the

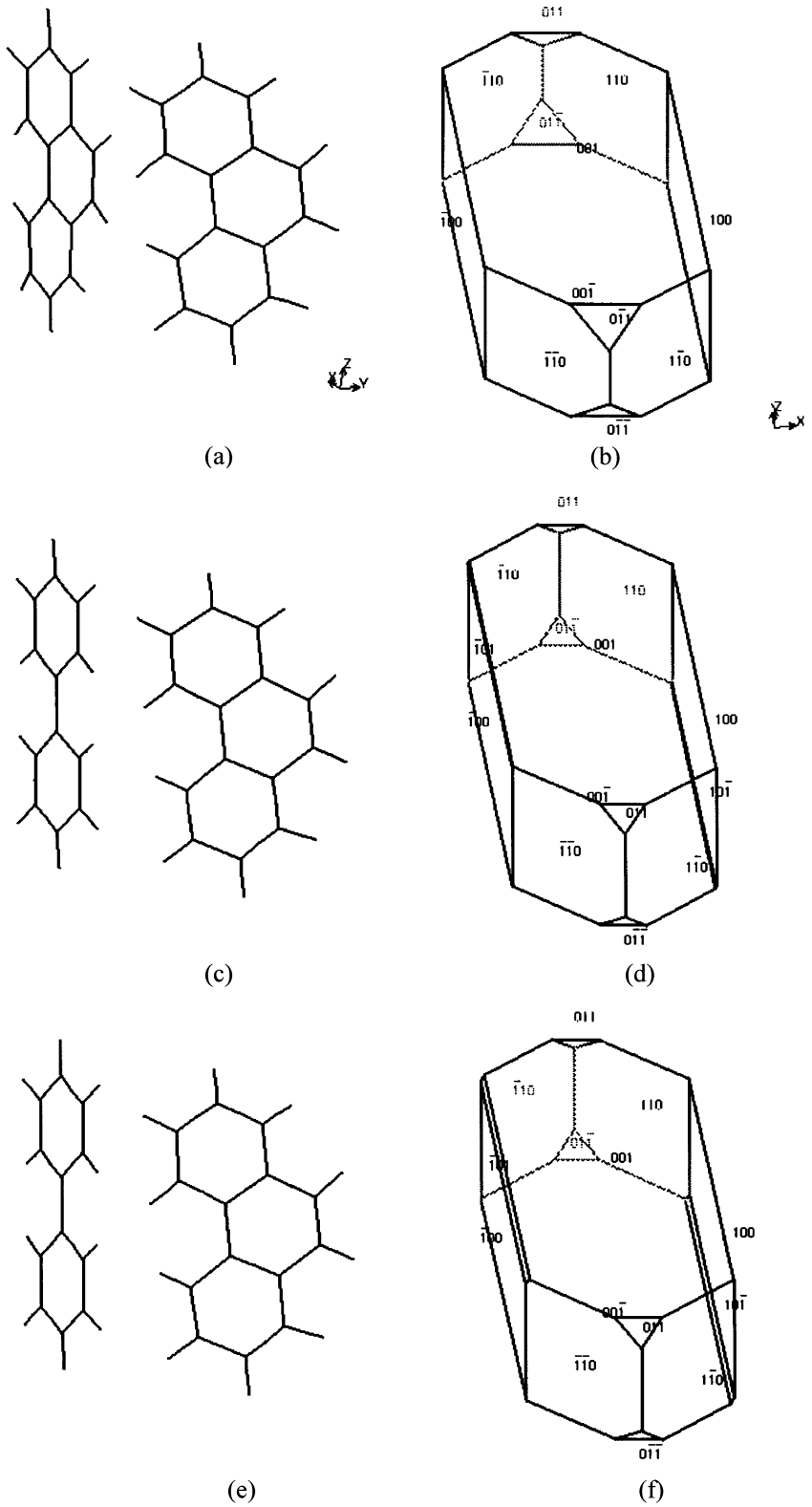

Figure 4. The effects of biphenyl on phenanthrene: (a) pure phenanthrene unit cell ($Z = 2$); (b) morphology of pure phenanthrene; (c) unrelaxed biphenyl additive in host unit cell; (d) morphology associated with components in panel c; (e) relaxed biphenyl additive in host unit cell; (f) morphology associated with components in panel e.

(110) faces.[25] This is predicted by both the rigid fit and minimization models with little difference between the simulated crystals (see Figure 3d,f). However, Table 3 shows how only after relaxation has been applied (compare Figure 3, parts a and e) do the (110) faces become the most favorable site for biphenyl incorporation (i.e., lowest Δb values), in agreement with experiment, while the results for the unrelaxed biphenyl molecule inaccurately suggest that $(11\bar{1})$ faces are preferred. Note also that fewer vacancies (N_v) are required, when the additive is allowed to relax its orientation, indicating that the latter calculation is more realistic, while the lower value of E_{att}'' for (110) obtained before minimization is simply the result of more vacancies being created than necessary with an attendant loss of energy and lowering of E_{att}''.

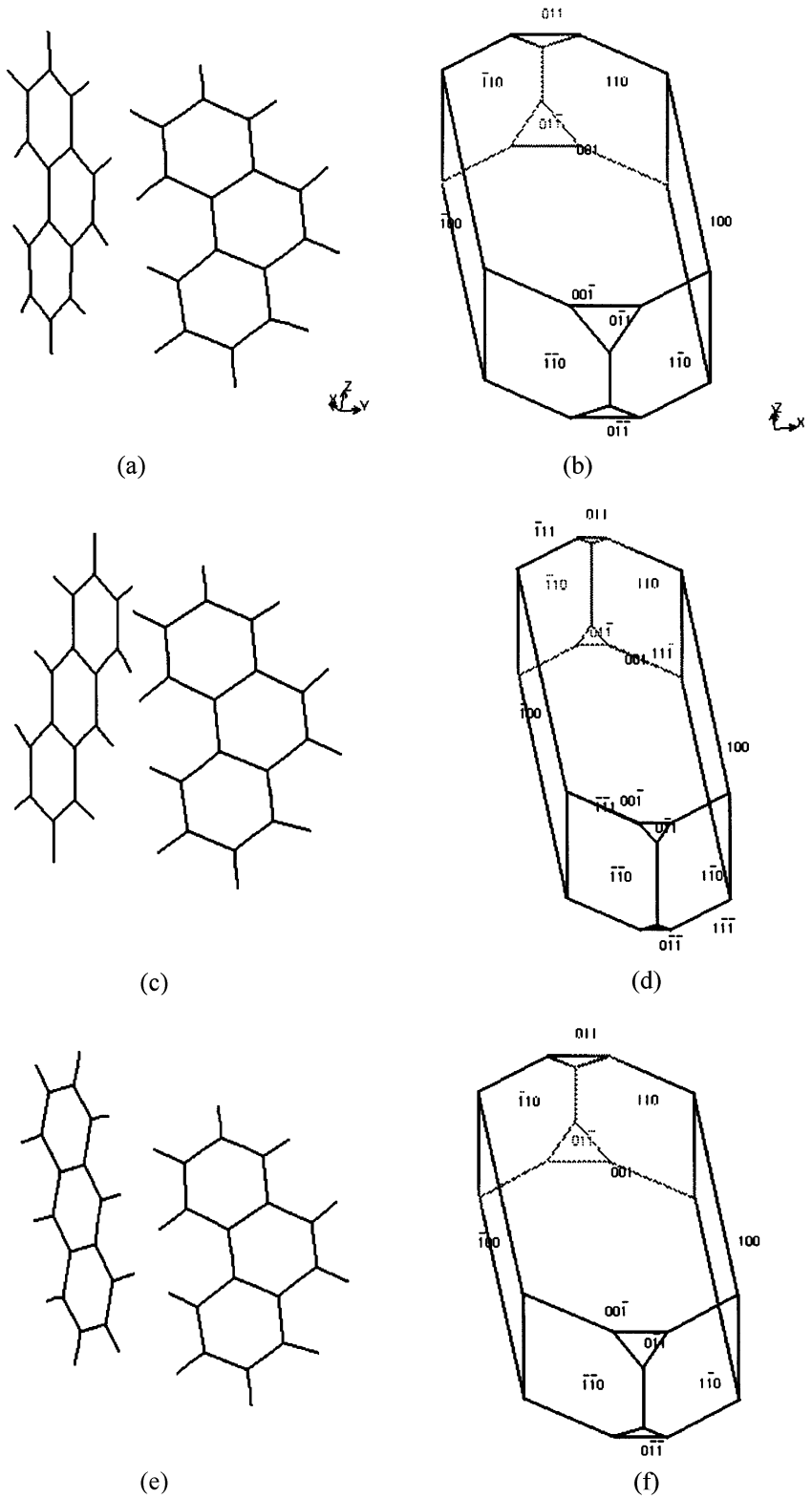

Figure 5. The effects of anthracene on phenanthrene: (a) pure phenanthrene unit cell ($Z = 2$); (b) morphology of pure phenanthrene; (c) unrelaxed anthracene additive in host unit cell; (d) morphology associated with components in panel c; (e) relaxed anthracene additive in host unit cell; (f) morphology associated with components in panel e.

3.2. The Effect of Biphenyl Impurity on the Phenanthrene Crystal Morphology. The minimization of biphenyl within the phenanthrene[26] lattice has little effect on the energy parameters, as shown in Table 4, implying the rigid additive orientation was already very close to the global minimum position. This is illustrated graphically by the similarity of Figure 4, parts c and e. Correspondingly, both binding energies and the simulated crystals (based on E_{att}'' values, Figure 4d, f) are also very similar, although the (001) faces decrease in importance (lower E_{att}'') with the impurity present and the (10$\bar{1}$) faces increase in importance.

3.3. The Effect of Anthracene Impurity on the Phenanthrene Crystal Morphology. Figure 5 clearly shows how, in contrast to biphenyl, the molecular orientation of the rigidly

TABLE 4: Changes in Binding Energy (Δb) and Attachment Energies (E_{att} for host, E_{att}'' for host + additive, kcal mol^{-1}) for Biphenyl and Anthracene Additives in a Phenanthrene Crystal before and after Relaxation[a]

	+ biphenyl (unrelaxed)		+ biphenyl (relaxed)		+ anthracene (unrelaxed)			+ anthracene (relaxed)			pure host
(*hkl*)	Δb	E_{att}''	Δb	E_{att}''	Δb	N_V[b]	E_{att}''	Δb	N_V[b]	E_{att}''	E_{att}
001	3.14	−5.30	3.14	−5.37	54.32	1	−4.52	1.09	2	−4.92	−5.79
10$\bar{0}$	1.66	−6.75	1.72	−6.87	2.50	2	−5.15	1.04	2	−7.48	−8.74
10$\bar{1}$	1.57	−9.15	1.49	−9.14	23.15	1	−7.56	6.27	0	−10.87	−11.23
0$\bar{1}$1	2.51	−14.77	2.48	−14.78	52.51	1	−13.85	1.14	2	−15.18	−16.75
011	1.58	−13.73	1.57	−13.92	1.29	2	−12.08	1.04	2	−15.03	−16.75
110	1.81	−12.07	1.84	−12.14	1.20	2	−10.10	2.80	1	−13.15	−14.70

[a] Results are given only for observed faces and for the asymmetric unit associated with the lowest Δb value. [b] N_V indicates the number of molecules replaced by vacancies; for biphenyl, $N_V = 0$.

fitted anthracene[27] (Figure 5c) is considerably shifted on relaxation (Figure 5e). This equates to a lowering of E_{cr} for the host/additive complex on minimization of 3.8 kcal mol^{-1} with anthracene present compared to only 0.05 kcal mol^{-1} with biphenyl (see Table 2). The morphological impact of anthracene on phenanthrene is, however, minor (compare Figure 5, parts d and f).

The importance of the relaxation process is further demonstrated by the Δb values given in Table 4. After relaxation, it can be seen that the anthracene molecule is now able to adsorb on all six observed faces ($\Delta b < 10$ kcal mol^{-1}) compared with only three faces for the treatment employing an unrelaxed additive molecule.

Experimental segregation data have shown that anthracene incorporates more extensively into phenanthrene crystals than biphenyl.[22] The energetic calculation results support this. First, E_{cr} for phenanthrene/anthracene is notably lower (and consequently segregation into the host crystal more favorable) than that for phenanthrene/biphenyl. Second, anthracene is preferentially incorporated (i.e., Δb is lower) for four of the six observed faces compared to biphenyl, while the Δb values imply a value of $K > 1$ for anthracene and $K < 1$ for biphenyl, as experiment[22] suggests.

4. Conclusions

Within the speciality chemicals industry, there are ever-more stringent requirements for products with low impurity levels and for the design of synthetic processes that avoid by-products, which segregate poorly. Accordingly, we have developed a robust computational methodology for particle shape prediction, which treats molecular crystals in the presence of an additive, and have demonstrated that the approach can be extended in a semiquantitative manner for predicting impurity segregation effects. The methodology has been applied to a series of benchmark impurity/host systems. In comparison to the previous approximation in which an additive molecule was placed in a fixed position based on molecular similarity with the host molecule, binding energy calculations that allow relaxation of the impurity within the host lattice have enabled the prediction of a more realistic estimate of impurity compatibility with both the host crystal lattice and individual crystal surface planes. The binding and surface attachment energies thus obtained have allowed, respectively, an estimation of the bulk impurity segregation coefficient for organic particulate solids and the simulation of their impurity-mediated crystal habit modification.

In respect of the aromatic systems studied here, the relaxation of biphenyl within a naphthalene lattice altered the binding energetics in such a manner as to correctly favor the (110) faces as the preferable sites for impurity incorporation, as observed by experiment, while the minimization of both biphenyl and anthracene within a phenanthrene lattice successfully mimicked experimental segregation data showing the more favorable incorporation of the latter material.

In addition to its application to simple van der Waals systems, similar to those studied here, the computational model has the potential to be applied to a wide variety of other more complex materials. Future work and further developments are therefore likely to include: (a) addressing the complex and distorting effect inherent in binding energy calculations involving hydrogen-bonded systems, in which a rigid fit produces too many vacancies to estimate E_{att}'' values accurately; (b) assessing solvent incorporation upon crystallization by considering the solvent molecule as an impurity and using surface relaxation techniques to obtain the optimum host surface structures or the optimum solvent binding sites (this strategy could also be used to model additives that are not "tailor-made"; (c) relaxation of both the impurity and its local crystal lattice environment to produce a closer approximation of the physical reality (this would be of particular use to enhance the simulation of the effects of so-called "blocker additives", for which the introduction of vacancies is currently necessary).

While the work presented here centers around applications improving process and product impurity and habit control, its extension to the generic area of crystallization inhibition, that is, via the selective design of additive-species' stereochemistry in a manner that could allow growth inhibition simultaneously on a number of crystallographically distinct (*hkl*) faces, is also feasible and constitutes an active area of our group research program. Against these objectives, a range of computational tools to address these issues are available within the Institute for Particle and Engineering Science, notably those involving Monte Carlo, systematic search, and genetic algorithm methods,[28,29] which are backed by an extensive resource of experimental data on the kind of systems studied and proposed here.

Acknowledgment. This work has been funded by an EPSRC/ROPA award (Grant GR/M/78052), which the authors gratefully acknowledge. We are also grateful to John Sherwood (University of Strathclyde, Glasgow, U.K.) and Will Wood (Syngenta, Huddersfield, U.K.) who, respectively, provided the stimulus for this work in terms of its relation to experiment and the work's industrial application.

References and Notes

(1) (a) Clydesdale, G.; Roberts, K. J.; Docherty, R. *Comput. Phys. Commun.* **1991**, *64*, 331. (b) Clydesdale, G.; Roberts, K. J.; Docherty, R. *J. Cryst. Growth*, **1996**, *166*, 78. (c) Clydesdale, G.; Roberts, K. J.; Docherty, R. *QCPE Bulletin*, QCPE Program no. 670; Quantum Chemistry Program Exchange, Indiana University: Bloomington, IN, 1996; Vol. 16, Issue 3, p 1; (d) *HABIT2000*. Unpublished results.

(2) Clydesdale, G.; Roberts, K. J.; Walker, E. M. In *Molecular Solid State: Synthesis, Structure, Reactions and Applications, Volume 2, Theoreti-*

cal Aspects and Computer Modelling; Gavezotti, A., Ed.; Wiley: Chichester, U.K., 1996; Chapter 7, p 506. Clydesdale, G.; Docherty, R.; Roberts, K. J. In *Colloid and Surface Engineering: Controlled Droplet, Bubble and Particle Formation*; Wedlock, D., Ed.; Butterworth-Heinemann: London, 1993; p 95; Clydesdale, G.; Roberts, K. J. In *Science and Technology of Crystal Growth. Lectures Given at the Ninth International Summer School on Crystal Growth, June 11−15, 1995*; van der Eerden, J. P., Bruinsma, O. S. C., Eds.; Kluwer Academic Press: Dordrecht, The Netherlands, 1995; p 367.

(3) Lahav, M.; Berkovitch-Yellin, Z.; van Mil, J.; Addadi, L.; Idelson, M.; Leiserowitz, L. *Isr. J. Chem.* **1985**, *25*, 353.

(4) Addadi, L.; Berkovitch-Yellin, Z.; Weissbuch, I.; Lahav, M.; Leiserowitz, L. *Top. Stereochem.* **1986**, *16*, 1−85.

(5) Berkovitch-Yellin, Z. *J. Am. Chem. Soc.* **1985**, *107*, 8239.

(6) Hartman, P.; Bennema, P. *J. Cryst. Growth* **1980**, *49*, 145.

(7) Gibbs, J. W. *Trans. Acad. Conn.* **1985**, 3. See also *The Equilibrium of Heterogeneous Substances (Scientific Papers, Vol. 1)*; Longmans Green: New York, 1928 and *Collected Works*; Longmans Green: New York, 1906.

(8) Wulff, G. *Z. Kristallogr.* **1901**, *34*, 499.

(9) *CERIUS molecular modelling software for materials research*, version 2.0; Molecular Simulations Inc.: Burlington, MA, and Cambridge, U.K.

(10) Docherty, R. Modelling the Morphology of Molecular Crystals. Ph.D. Thesis, University of Strathclyde, Glasgow, U.K., 1989. Roberts, K. J.; Yoon, X. S.; Sherwood, J. N.; Docherty, R. *Chem. Mater.* **1994**, *6*, 1099.

(11) Clydesdale, G.; Roberts, K. J.; Lewtas, K.; Docherty, R. *J. Cryst. Growth* **1994**, *141*, 443.

(12) Clydesdale, G.; Roberts, K. J.; Docherty, R. *Crystal Growth of Organic Materials*; Myerson, A., Green, D. A., Meenan, P., Eds.; Conference Proceedings Series 1054−7487; American Chemical Society: Washington DC, 1996; pp 43−52.

(13) Clydesdale, G. The Development of Predictive Approaches for Modelling the Polymorphic Stability and Crystal Habit of Normal Alkanes and Other Molecular Crystals. Ph.D. Thesis, University of Strathclyde, Glasgow, U.K., 1991.

(14) Clydesdale, G.; Docherty, R.; Roberts, K. J. *J. Cryst. Growth* **1994**, *135*, 331. Clydesdale, G.; Roberts, K. J.; Lewtas, K. *Mol. Cryst. Liq. Cryst.* **1994**, *248*, 243.

(15) Bladon, P.; Breckinridge, R. *INTERCHEM 6.1*; QCPE Bulletin; Quantum Chemistry Program Exchange, Indiana University: Bloomington, IN, 1994; Vol. 14, Issue 3, p 47.

(16) Williams, D. E. *J. Chem. Phys.* **1966**, *45*, 3370.

(17) Kitaigorodskii, A. I. *Tetrahedron* **1961**, *14*, 230.

(18) Buckingham, R.; Corner, J. *Proc. R. Soc. London* **1947**, *189*, 118.

(19) Stewart, J. *Comput.-Aided Mol. Des.* **1990**, *4*, 1.

(20) Williams, D. E. *Acta Crystallogr., Sect. A* **1972**, *28*, 629−635.

(21) Press, W. H.; Teukolsky, S. A.; Vetterling, W. T.; Flannery, B. P. *Numerical Recipies in FORTRAN 77, The Art of Scientific Computing*, 2nd ed.; Cambridge University Press: Cambridge, U.K., 1996; p 421.

(22) (a) McArdle, B. J.; Sherwood, J. N. *Chem. Ind.*, **1985**, *April*, 269. (b) McArdle, B. J.; Sherwood, J. N.; Damask, A. C. *J. Cryst. Growth* **1987**, *22*, 193.

(23) Trotter, J. *Acta Crystallogr.* **1961**, *14*, 1135.

(24) Ponomarev, V. I.; Filipenko, O. S.; Atovmyan, L. O. *Kristallographia* **1976**, *21*, 392.

(25) Jetten, L. A. M. J. Ph.D. Thesis, University of Nijmegen, The Netherlands, 1983.

(26) Petricek, V.; Cisarova, I.; Hummel, L.; Kroupa, J.; Brezina, B. *Acta Crystallogr., Sect. B* **1990**, *46*, 830.

(27) Mason, R. *Acta Crystallogr.* **1964**, *17*, 547.

(28) Hammond, R. B.; Roberts, K. J.; Docherty, R.; Edmondson, M.; Gairns, R. *J. Chem. Soc., Perkin Trans.* **1996**, *2*, 1527.

(29) Hammond, R. B.; Roberts, K. J.; Docherty, R.; Edmondson, M. *J. Phys. Chem. B* **1997**, *101*, 6532.